Reprinted from

JAPANESE JOURNAL OF
APPLIED
PHYSICS

REGULAR PAPER

Evaluation of Rate of Change in Thickness of Heart Wall by Measuring Time Variation of Ultrasonic Integrated Backscatter during a Cardiac Cycle

Hiro Shida, Hideyuki Hasegawa, and Hiroshi Kanai

Jpn. J. Appl. Phys. **51** (2012) 07GF05

Japanese Journal of Applied Physics **51** (2012) 07GF05 **REGULAR PAPER**
DOI: 10.1143/JJAP.51.07GF05

Evaluation of Rate of Change in Thickness of Heart Wall by Measuring Time Variation of Ultrasonic Integrated Backscatter during a Cardiac Cycle

Hiro Shida[1], Hideyuki Hasegawa[1,2], and Hiroshi Kanai[1,2*]

[1]*Graduate School of Biomedical Engineering, Tohoku University, Sendai 980-8579, Japan*
[2]*Graduate School of Engineering, Tohoku University, Sendai 980-8579, Japan*

Received November 18, 2011; accepted February 27, 2012; published online July 20, 2012

Integrated backscatter (IB) from the heart wall is gaining attention as a quantitative tissue characterization method and the cyclic variation (CV) in IB during a cardiac cycle offers potential for the evaluation of myocardial contractility. Since there is large motion in the heart wall owing to the heartbeat, in the conventional method, the position of the region of interest (ROI) for calculating the IB is manually assigned in each frame during one cardiac cycle. Moreover, the change in the size of the ROI during contraction and relaxation of the myocardium is not considered. In this study, the *phased tracking method* was applied to multiple points in the heart wall for automatic tracking of the position and size of the ROI and, then, IB in the same site of the heart wall was measured in each frame by improving temporal resolution and spatial resolution in the axial direction. As a result, cyclic variations, which differed site by site, were found. Furthermore, the rate of change in thickness was estimated by using the interference cycle obtained by applying the discrete Fourier transform (DFT) to IB signals. According to the results, the rate of change in thickness estimated using the interference cycle of IB was in good agreement with that estimated by the *phased tracking method*. These results indicate the possibility of estimating the rate of change in thickness using the IB signal.

1. Introduction

For the diagnosis of heart disease such as myocardial infarction, hypertrophic cardiomyopathy, and dilated cardiomyopathy, noninvasive myocardial tissue characterization is important. Previously, the echogenicity of the heart wall of patients with previous myocardial infarction and hypertrophic cardiomyopathy in the ultrasonic B- and M-mode images was known to be high.[1–6] However, quantitative characterization of myocardial tissue has not yet been realized.

Integrated backscatter (IB) from the heart wall, which is able to measure the phenomenon in a region of a size less than the ultrasonic wavelength of about 500 μm, is gaining attention as a quantitative tissue characterization method. The IB is obtained by averaging the ultrasonic scattering power from a region in tissues. In previous studies, it was found that IB from the myocardium exhibits cyclic variation during one cardiac cycle,[7–9] i.e., the magnitude decreases during systole and increases during diastole. The magnitude of such variation is reduced by ischemia.[10] These results suggest that the cyclic variation in ultrasound IB during one cardiac cycle offers potential for the evaluation of myocardial contractility. Thus, analysis of the cyclic variation of ultrasonic IB has been established as a noninvasive and sensitive method for evaluating intrinsic left ventricular (LV) contractile performance and for detecting myocardial viability.[11–14]

Since there is large motion due to the heartbeat in the heart wall, in conventional measurement, the position of the region of interest (ROI) for detecting IB is manually assigned in each frame during one cardiac cycle. Furthermore, the thickness of the heart wall changes during contraction and relaxation of the myocardium. However, the change in size of the ROI is completely ignored in conventional measurement of IB. Thus, it is difficult to obtain IB from the same site during one cardiac cycle.

It is reported that a patient with myocardial infarction shows a low CV in IB and a high baseline value of IB. Naito *et al.* investigated the change in IB under doses of dobutamine and β blocker.[15] They showed that CV in IB was increased by dobutamine and decreased by β blocker. They discussed that such changes in IB were caused by the increased contractility of the myocardium caused by dobutamine and the decreased contractility caused by β blocker. Masuyama *et al.* showed that the CV of a patient with hypertrophic cardiomyopathy was significantly smaller than that of a healthy subject.[3] They mentioned that the myocardial contractility of a patient with hypertrophic cardiomyopathy was decreased by tangled myocardial fiber. Furthermore, Hoyt *et al.* reported that there was a correlation between the amount of hydroxyproline, which is the main component of fibrous tissue in the myocardium, and the baseline value of IB.[16]

To improve the spatial resolution in the estimation of the myocardial displacement, Kanai *et al.* proposed the *phased tracking method*, which enables the detection of small vibrations in the heart wall.[17] This method was applied to multiple points preset in the LV wall along an ultrasonic beam so that the spatial distribution of velocities at those points is simultaneously obtained.[18,19] Furthermore, this method was applied to other applications, such like the measurements of heart wall vibrations induced by external actuation[20] and the strain waveform of the radial arterial wall.[21]

There are several studies on the measurement of IB with tracking of myocardial motion. Bai *et al.* measured cyclic variation in IB by tracking myocardial motion using a speckle tracking technique.[22] They showed that the normal myocardium and the infarcted myocardium can be differentiated by cyclic variation in IB measured by their method. Sekioka *et al.* used a tracking method based on ultrasonic RF echoes for the measurement of IB.[23] They mentioned that differences between IBs of hearts of healthy subjects and patients with myocardial infarction were enhanced by tracking myocardial motion. However, the temporal resolutions in these previous studies are not sufficient to detect the high-frequency variation in IB that is investigated in the present study. Therefore, the *phased tracking method*, which can measure myocardial motion accurately at a high temporal resolution, was used in the present study to measure IB from the myocardium.

*E-mail address: kanai@ecei.tohoku.ac.jp

In this study, by applying the *phased tracking method*, which estimates the displacement of an object with a high degree of accuracy using the phase shift of the RF signal, an ROI assigned in the heart wall along an ultrasonic beam is accurately tracked. By setting the ROI between two adjacent points along the beam, the instantaneous position and the size of the ROI corresponding to displacement and change in thickness of the heart wall are automatically determined. Thus, it is possible to measure the IB in the same site of the heart wall in each frame with better time resolution and spatial resolution in the axial direction. Since the spatial resolution and time resolution were significantly improved, rapidly varying components were observed in the IB signal. Such rapidly varying components highly depend on the strain rate of the heart wall and these components result from the interference between the ultrasonic waves reflected by scatterers. By applying the proposed method to an *in vivo* experiment, the interference cycle of the IB signal was calculated to estimate the rate of change in the thickness of the heart wall.

2. Principles

2.1 Detection of IB from the same site in the heart wall

Figure 1 illustrates the proposed method for calculating the IB. At the time of electrocardiographic R-wave, N layers with a thickness of $\Delta d = 2463\,\mu\text{m}$ were assigned in the interventricular septum (IVS) from the right ventricular (RV) side to the left ventricular side along an ultrasonic beam with intervals of $\Delta d/4 = 616\,\mu\text{m}$ and then, the IB was calculated in each layer in one cardiac cycle. The thickness Δd was determined from the duration of an ultrasonic pulse transmitted from the ultrasonic probe. The IB signal $IB_i(t)$ of the i-th layer from the RV surface ($i = 0$) at time t is given by[24]

$$IB_i(t) = 10\log_{10}\frac{1}{\Delta d(t)}\int_{x_{1i}(t)}^{x_{2i}(t)} |z(t,\xi)|^2\, d\xi, \tag{1}$$

$$\Delta d(t) = x_{2i}(t) - x_{1i}(t), \tag{2}$$

where $z(t,\xi)$ is the quadrature demodulated signal of the ultrasonic pulse scattered by the object at depth position $x = \xi$ at time t, and $x_{1i}(t)$ and $x_{2i}(t)$ are the top and bottom of the i-th layer ($i = 0, 1, 2, \ldots, N-1$), respectively.

2.2 Interference cycle of IB and rate of change in thickness

In the present study, the interference cycle of the IB signal in the time (frame) direction is estimated. When intramyocardial scatterers move in response to the changes in thickness of the heart wall, the interference state of multiple scattered waves varies. If the distance between two scatterers is varies owing to the change in thickness, the rate of change in the distance of scatterers, i.e., the rate of change in thickness, is determined by estimating the cycle of the change in IB. Figure 2(a) illustrates the case of two scatterers. Ultrasonic echoes from scatterer A and scatterer B in the n-th frame and $(n+1)$-th frame are given by

$$\begin{cases} S_{\text{A}}(t;n) = \cos(2\pi f_0 t), \\ S_{\text{B}}(t;n) = \cos\left[2\pi f_0\left(t + \dfrac{2\delta d}{c_0}\right)\right], \end{cases}$$

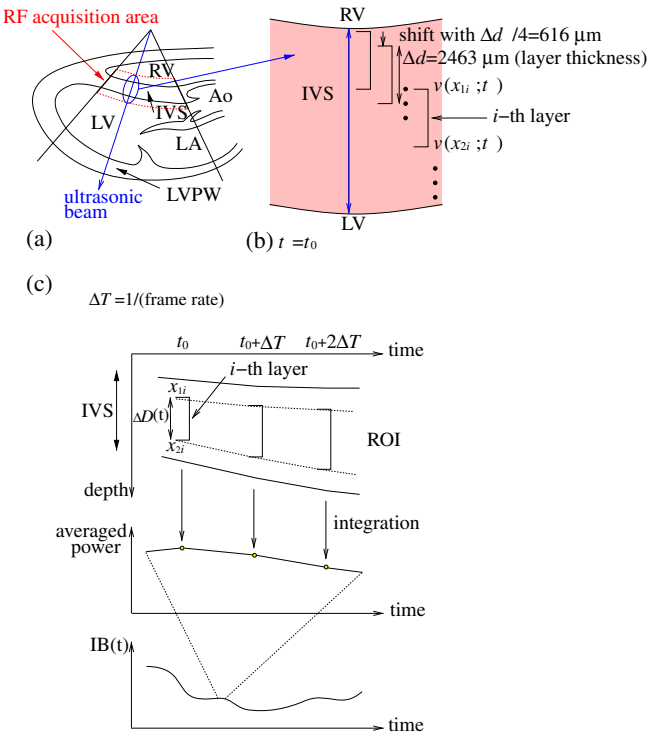

Fig. 1. (Color online) (a) RF signal acquisition in the parasternal longitudinal-axis view of the LV. (b) Method of assigning layers along an ultrasonic beam at $t = t_0$. (c) Illustration of the proposed method for calculating the IB by tracking the instantaneous position and thickness of the ROI.

$$\begin{cases} S_{\text{A}}(t;n+1) = \cos(2\pi f_0 t), \\ S_{\text{B}}(t;n+1) = \cos\left\{2\pi f_0\left[t + \dfrac{2(\delta d + \Delta d_i)}{c_0}\right]\right\}, \end{cases}$$

where f_0 is the ultrasonic center frequency and c_0 is the acoustic velocity. Thus, the phase difference $\Delta\theta_i$ due to the change in thickness Δd_i between two frames is given by

$$\Delta\theta_i = 2\pi f_0 \frac{2\Delta d_i}{c_0}. \tag{3}$$

Therefore, the interference cycle T_i is given by substituting $\Delta\theta_i = 2\pi\Delta T/T_i$ as follows:

$$T_i = \frac{c_0}{2f_0}\cdot\frac{\Delta T}{\Delta d_i}. \tag{4}$$

As shown in eq. (4) and Fig. 2(a), $\Delta d_i/\Delta T$ indicates the rate of change in distance of scatterers, i.e., the rate of change in thickness. Then, the average rate of change in thickness v_i in each layer is given by

$$v_i = \frac{c_0}{2f_0}\cdot\frac{1}{T_i}, \tag{5}$$

$$= \frac{c_0}{2f_0}\cdot f_i, \tag{6}$$

where f_i is the interference frequency. Also, the rate of change in thickness obtained by the *phased tracking method* v_{ip} is given by[25]

$$v_{\text{p},i} = |v(x_{2i};t) - v(x_{1i};t)|, \tag{7}$$

where $v(x_{2i};t)$ and $v(x_{1i};t)$ are the velocities of the top and bottom of the i-th layer, respectively. The *phased tracking method* requires two points along an ultrasonic beam to

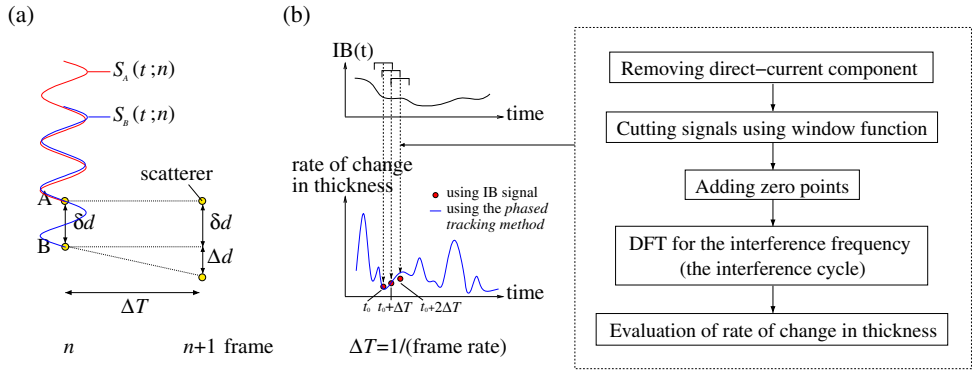

Fig. 2. (Color online) (a) Relationship between interference cycle and rate of change in thickness in the case of two scatterers. (b) Illustration and schematic procedure of calculation of rate of change in thickness proposed in this study.

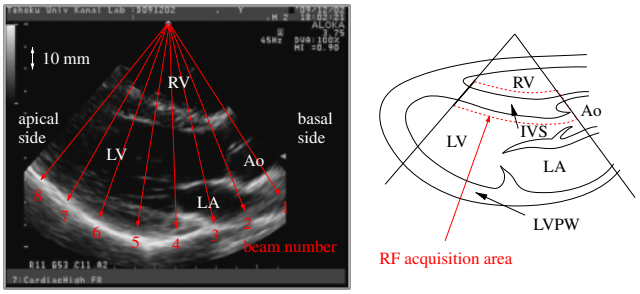

Fig. 3. (Color online) Cross-sectional image of the left ventricle in the long-axis view obtained by conventional echocardiography for a healthy 24-year-old male. The red arrows show the direction of the eight ultrasonic beams used for calculation of IB in the IVS.

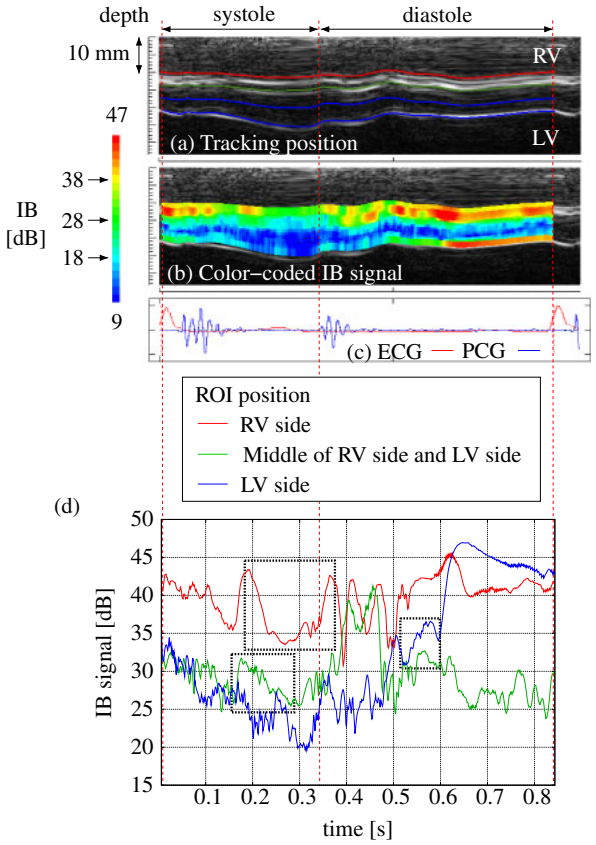

Fig. 4. (Color online) *In vivo* experimental results for the IVS along beam 5. (a) The tracking lines for RV side (red line), middle of IVS (green line), and LV side (blue line) overlaid on the M-mode image. (b) Color-coded image of IB signals. (c) ECG (red line) and PCG (blue line). (d) IB signals for RV side (red line), middle of IVS (green line), and LV side (blue line).

estimate the rate of change in thickness. In contrast, the interference cycle of IB, which corresponds to the change in thickness, can be estimated using each single depth point. In this study, the interference cycle was obtained by Fourier transform in accordance with the process in Fig. 2(b). To identify peaks in the frequency spectrum of the IB signal, it is necessary to remove the direct-current component from IB signals and zero points (total 512 points) were added to improve the frequency resolution. Then, the rate of change in thickness was calculated using the interference frequency of IB and the *phased tracking method*.

3. *In vivo* Experimental Results

3.1 Discrimination of interference component from noise

Figure 3 shows a typical cross-sectional image (transthoracic parasternal longitudinal-axis view) of the heart obtained from a healthy 24-year-old male. The figure on the right-hand side of Fig. 3 shows the RF acquisition area. The RF data were acquired at a frame rate of 888 Hz using a 3.75-MHz sector-type probe of ultrasonic diagnostic equipment (ALOKA SSD-6500). The sampling frequency of the RF signal was 15 MHz. Figure 4 shows IB signals of the RV side (red line), the middle (green line), and the LV side (blue line) of the IVS along beam 5. In Fig. 4, there is cyclic variation in each ROI, which is the same as that reported previously (the magnitude decreases during systole and increases during diastole). During diastole, the myocardial fiber was depressed and the orientation of the fibers became almost parallel, and the incident angle of the ultrasound becomes perpendicular to almost all the fibers. Thus, the magnitude of the integrated backscatter increased during diastole. This is opposite in systole, i.e., there are various fiber orientations. In addition to the conventional cyclic variation, the rapidly varying components, which are thought to be due to interference between the ultrasonic waves reflected by scatterers, are apparent during one cardiac cycle. Figures 5(a)–5(c) are the enlarged views of IB signals in different periods (black dotted lines for each ROI in Fig. 4). IB signals obtained by *in vivo* measurement

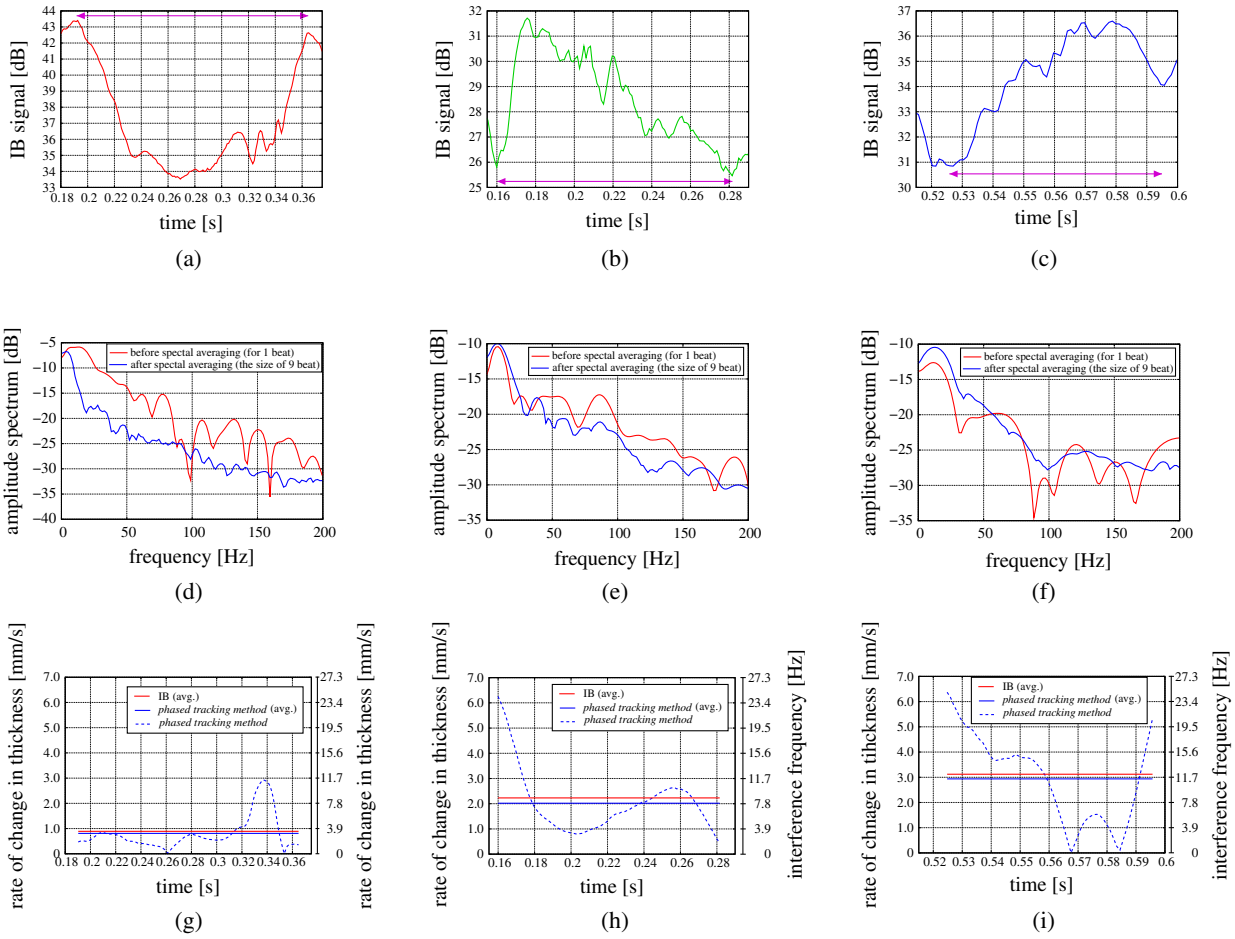

Fig. 5. (Color online) Measured rates of change in thickness obtained using interference frequency of IB signal within the period of black dotted line for each ROI in Fig. 4. (a) Enlarged view of IB signal of RV side. (b) Enlarged view of IB signal of middle of IVS. (c) Enlarged view of IB signal of LV side. (d) Amplitude spectrum of IB signal in (a). (e) Amplitude spectrum of IB signal in (b). (f) Amplitude spectrum of IB signal in (c). (g) Average rate of change in thickness in the RV side. (h) Average rate of change in thickness of middle of IVS. (i) Average rate of change in thickness in the LV side.

contained low-frequency and high-frequency components. To examine these components, the spectra of IB signals were averaged.

Figures 5(d)–5(f) show the amplitude spectra obtained for IB signals in Figs. 5(a)–5(c) by applying the DFT with Hanning windows with lengths of 176 ms (RV side), 108 ms (middle of IVS), and 64 ms (LV side). In Figs. 5(d)–5(f), the red line indicates the spectrum before averaging (for 1 beat) and the blue line indicates the spectrum after averaging (for 9 beats). For each ROI, frequency components at over 50 Hz were considered to be noise from the average spectrum. Thus, the low-frequency components in Figs. 5(d)–5(f) are considered to correspond to the interference component of scatterers, i.e., the rate of change in thickness. From the average spectrum, the frequencies of peaks were calculated to be 5.7 Hz (RV side), 8.7 Hz (middle of IVS), and 12.1 Hz (LV side) and these peaks were identified as interference frequencies. Each interference frequency corresponds to the cycle indicated by the arrow on the IB signals in Figs. 5(a)–5(c). Figures 5(g)–5(i) show the average rate of change in thickness within the analysis period estimated using the interference frequency of IB signals (red line) and the *phased tracking method* (blue line). The blue dotted line is the instantaneous rate of change in thickness within the analysis interval obtained by the *phased tracking method*. As shown in Figs. 5(g)–5(i), the values obtained by the two methods were nearly equal. This indicates the possibility of the proposed method for estimating the rate of change in thickness using the IB signal.

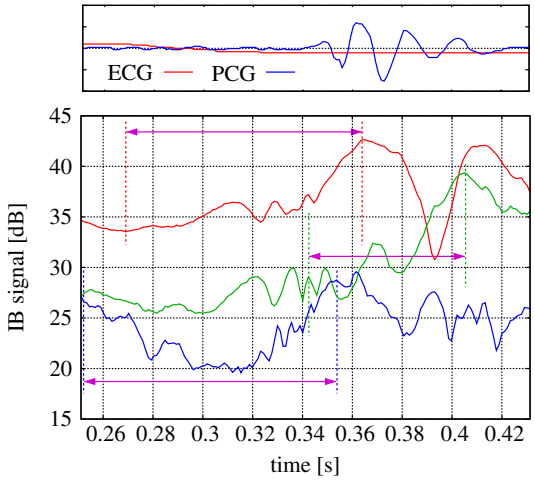

Fig. 6. (Color online) Enlarged view of IB signals in the period for frequency analysis around second heart sound (±90 ms).

3.2 Rates of change in thickness during same period and during one cardiac cycle

Figure 6 shows an enlarged view of IB signals during the

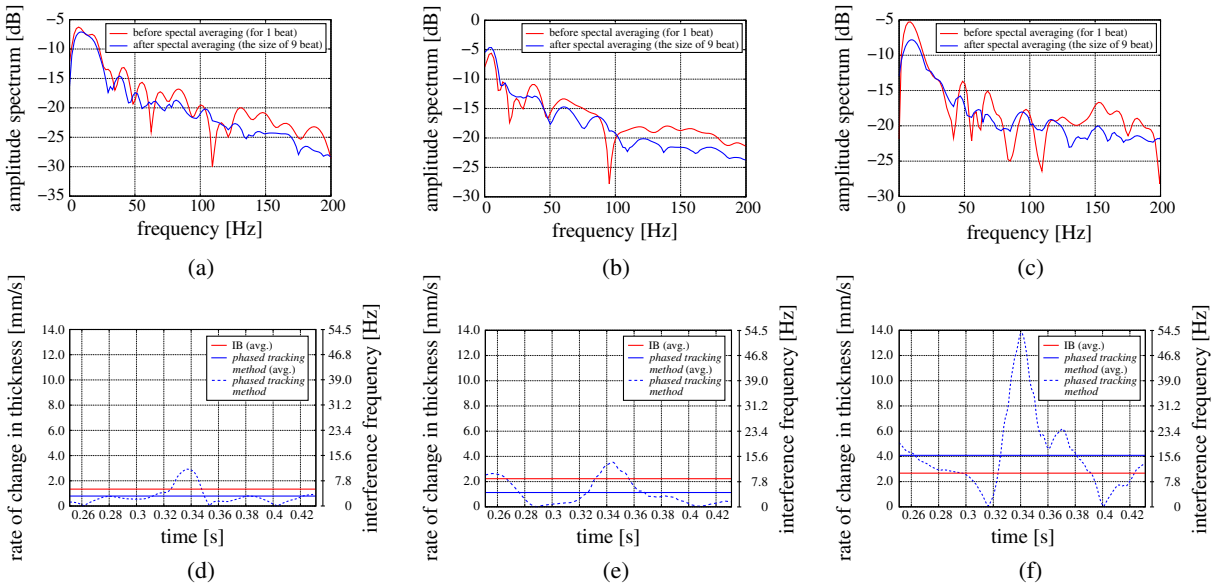

Fig. 7. (Color online) Measurement of rate of change in thickness obtained using interference frequency of IB signal in the period for frequency analysis around second heart sound (±90 ms). (a) Amplitude spectrum of IB signal in Fig. 6, RV side (red line). (b) Amplitude spectrum of IB signal of middle of IVS (green line). (c) Amplitude spectrum of IB signal in Fig. 5, LV side (blue line). (d) Average rate of change in thickness in the RV side. (e) Average rate of change in thickness of middle of IVS. (f) Average rate of change in thickness in the LV side.

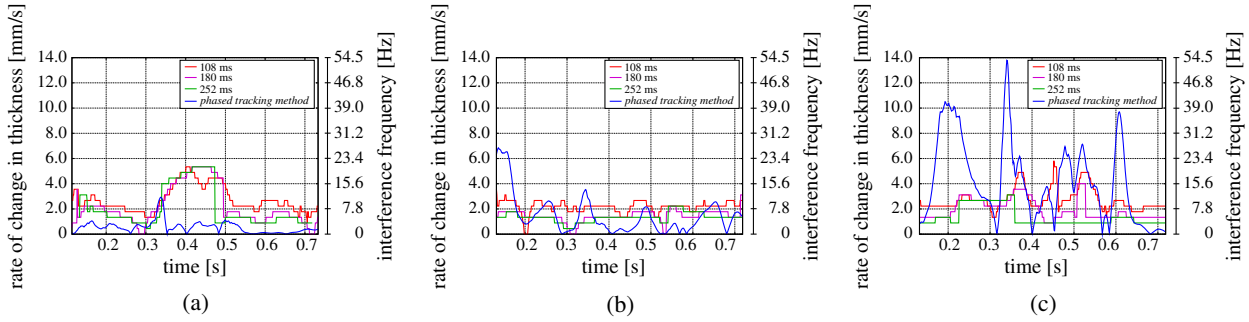

Fig. 8. (Color online) Comparison of instantaneous rates of change in thickness during one cardiac cycle using window lengths of 108 ms (red line), 180 ms (purple line), and 252 ms (green line) for frequency analysis. Instantaneous rate of change in thickness obtained by the *phased tracking method* is shown by the blue lines. (a) RV side. (b) Middle of IVS. (c) LV side.

period for frequency analysis around the second heart sound ±90 ms. Figures 7(a)–7(c) show the amplitude spectra of IB signals obtained in Fig. 6 by applying the DFT with a Hanning window with a length of 180 ms so that the distance between scatterers in the myocardium largely varies and the interference arises in each ROI, especially in the RV side. From the average spectrum, the interference frequencies were calculated at 5.2 Hz (RV side), 8.7 Hz (middle of IVS), and 10.4 Hz (LV side). Each interference frequency corresponds to the cycle indicated by the arrow on the IB signals in Fig. 6. Figures 7(d)–7(f) show the average rates of change in thickness within the analysis period obtained using the interference frequency of IB signals (red line) and the *phased tracking method* (blue line). The blue dotted line is the instantaneous rate of change in thickness within the analysis period obtained using the *phased tracking method*. As described in the previous section, the values obtained by the two methods are nearly equal, especially in the RV side. Furthermore, the average values of rates of change in thickness within the analysis period are summarized in Table I. Both rates of change in thickness obtained by the proposed method and the *phased tracking method* were larger in the LV side than the RV side. Such a tendency is in good agreement with previous reports.[26] From these results, the proposed method was shown to have potential for the estimation of the rate of change in thickness using the interference cycle of the IB signal.

Table I. Average values of rates of change in thickness obtained using two methods.

Method	ROI position	Rate of change in thickness (mm/s)
IB signal	RV	1.34
	Middle	2.23
	LV	2.67
Phased tracking	RV	0.79
	Middle	1.14
	LV	4.08

4. Discussion

As shown in the results in Figs. 7(d)–7(f) and Table I, a large window length is necessary when an ROI is assigned in the RV side to detect the interference between echos from scatterers, which move in response to the change in thickness of the heart wall. That is, a large window length is not indispensable for the LV side where the rate of change in thickness during one cardiac cycle is large. Also, myocardial lateral motion cannot be neglected when such a long window is used. Figure 8 shows the instantaneous rate of change in thickness during one cardiac cycle obtained using shorter and longer windows for frequency analysis. The results obtained by both the proposed method and the *phased tracking method* show a similar tendency (large change in thickness in the LV side). Also, it was found that the estimated values obtained by windows longer than 180 ms are very close to that obtained by the *phased tracking method* in the RV side and the middle of IVS. In contrast, the values obtained by windows shorter than 180 ms are very close to that obtained by the *phased tracking method* in the LV side. If the optimal window length is used in each frame and ROI position, it might be possible to estimate the rate of change in thickness with a high degree of accuracy.

5. Conclusion

In this study, we proposed a method for estimation of the rate of change in thickness using the IB signal. To examine the low-frequency component and high-frequency component, the spectra of IB signals were averaged and the interference components due to interference between the ultrasonic waves reflected by scatterers, which move in response to a change in thickness of the heart wall, were found in addition to the conventional cyclic variation. The interference frequency calculated by DFT in the same period reflected the well-known contractile and relaxant characteristics fairly well. Also, it was indicated that it might be possible to estimate the rate of change in thickness with a high degree of accuracy if the optimal window length is selected for each frame and ROI position. These results indicate that the proposed method have potential for the evaluation of the rate of change in thickness using the interference cycle of the IB signal.

1) A. K. Bhandari and N. C. Nanda: Am. J. Cardiol. **51** (1983) 817.
2) J. G. Miller, J. E. Perez, and B. E. Sobel: Prog. Cardiovasc. Dis. **28** (1985) 85.
3) T. Masuyama, F. S. Goar, T. Tye, G. Oppenheim, I. Schnittger, and R. Popp: Circulation **80** (1989) 925.
4) J. Naito, T. Masuyama, T. Mano, H. Kondo, K. Yamamoto, R. Nagano, Y. Doi, M. Hori, and T. Kamada: Am. Heart J. **131** (1996) 115.
5) M. R. Milunski, G. A. Mohr, K. A. Wear, B. E. Sobel, J. G. Miller, and S. A. Wickline: J. Am. Coll. Cardiol. **14** (1989) 462.
6) J. Naito, T. Masuyama, K. Yamamoto, T. Mano, H. Kondo, R. Nagano, Y. Doi, T. Morozumi, H. Ito, K. Fujii, M. Hori, and T. Kamada: Am. Heart J. **132** (1996) 54.
7) B. Barzilai, E. I. Madaras, B. E. Sobel, J. G. Miller, and J. E. Perez: Am. J. Physiol. **247** (1984) H478.
8) E. I. Madaras, B. Barzilai, J. E. Perez, B. E. Sobel, and J. G. Miller: Ultrason. Imaging **5** (1983) 229.
9) R. M. Glueck, J. G. Mottley, J. G. Miller, B. E. Sobel, and J. E. Perez: Circulation **68** (1983) III-330.
10) M. L. Marcus, R. E. Kerber, J. Ehrhardt, and F. M. Abboud: Circulation **52** (1975) 254.
11) S. A. Wickline, L. J. Thomas III, J. G. Miller, B. E. Sobel, and J. E. Perez: Circulation **72** (1985) 183.
12) S. A. Wickline, L. J. Thomas III, J. G. Miller, B. E. Sobel, and J. E. Perez: Circulation **74** (1986) 389.
13) S. Nozaki, A. N. DeMaria, G. A. Helmer, and H. K. Hammond: Circulation **92** (1995) 2676.
14) S. Takiuchi, H. Ito, K. Iwakura, Y. Taniyama, N. Nishikawa, T. Masuyama, M. Hori, Y. Higashino, K. Fujii, and T. Minamino: Circulation **97** (1998) 356.
15) J. Naito, T. Masuyama, T. Mano, K. Yamamoto, Y. Doi, H. Kondo, R. Nagano, M. Inoue, and M. Hori: Ultrasound Med. Biol. **22** (1996) 305.
16) R. H. Hoyt, S. M. Collins, D. J. Skorton, E. E. Ericksen, and D. Conyers: Circulation **71** (1985) 740.
17) H. Kanai, M. Sato, Y. Koiwa, and N. Chubachi: IEEE Trans. Ultrason. Ferroelectr. Freq. Control **43** (1996) 791.
18) H. Kanai, H. Hasegawa, N. Chubachi, Y. Koiwa, and M. Tanaka: IEEE Trans. Ultrason. Ferroelectr. Freq. Control **44** (1997) 752.
19) H. Kanai, Y. Koiwa, Y. Saito, I. Susukida, and M. Tanaka: Jpn. J. Appl. Phys. **38** (1999) 3403.
20) H. Kanai, H. Hasegawa, and K. Imamura: Jpn. J. Appl. Phys. **45** (2006) 4718.
21) K. Ikeshita, H. Hasegawa, and H. Kanai: Jpn. J. Appl. Phys. **50** (2011) 07HF08.
22) J. Bai, Y. Jiang, K. Ying, P. Zhang, and J. Shao: Ultrasonics **48** (2008) 394.
23) K. Sekioka, T. Kunisada, S. Tsuruoka, H. Ishii, W. Oyama, and T. Wakabayashi: Denshi Joho Tsushin Gakkai Ronbunshi D-II **J87-D-II** (2004) 98 [in Japanese].
24) H. Kanai, Y. Koiwa, S. Katsumata, N. Izumi, and M. Tanaka: Jpn. J. Appl. Phys. **42** (2003) 3239.
25) H. Yoshiara, H. Hasegawa, H. Kanai, and M. Tanaka: Jpn. J. Appl. Phys. **46** (2007) 4889.
26) T. Edvardsen, B. L. Gerber, J. Garot, D. A. Bluemke, J. A. C. Lima, and O. A. Smiseth: Circulation **106** (2002) 50.